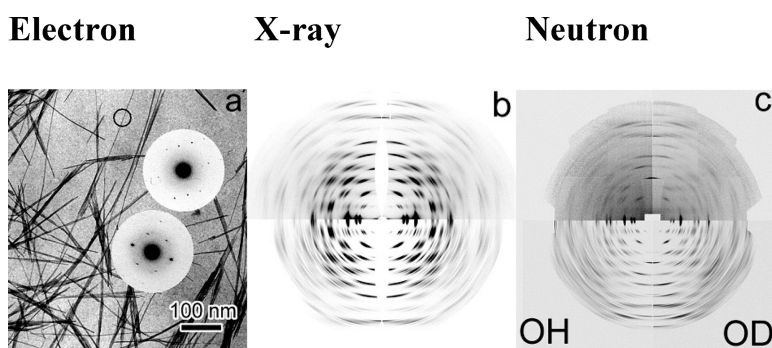


Crystal Structure and Hydrogen Bonding System in Cellulose I from Synchrotron X-ray and Neutron Fiber Diffraction

Yoshiharu Nishiyama, Junji Sugiyama, Henri Chanzy, and Paul Langan

J. Am. Chem. Soc., **2003**, 125 (47), 14300-14306 • DOI: 10.1021/ja037055w • Publication Date (Web): 05 November 2003

Downloaded from <http://pubs.acs.org> on March 30, 2009



More About This Article

Additional resources and features associated with this article are available within the HTML version:

- Supporting Information
- Links to the 25 articles that cite this article, as of the time of this article download
- Access to high resolution figures
- Links to articles and content related to this article
- Copyright permission to reproduce figures and/or text from this article

[View the Full Text HTML](#)

Crystal Structure and Hydrogen Bonding System in Cellulose I_α from Synchrotron X-ray and Neutron Fiber Diffraction

Yoshiharu Nishiyama,[†] Junji Sugiyama,[‡] Henri Chanzy,[§] and Paul Langan^{*||}

Contribution from the Department of Biomaterial Sciences, Graduate School of Agriculture and Life Science, the University of Tokyo, Yayoi 1-1-1, Bunkyo-ku, Tokyo 113, Japan, Wood Research Institute, Kyoto University, Uji, Kyoto 611-0011, Japan, Centre de Recherches sur les Macromolécules Végétales, CNRS, affiliated with the Joseph Fourier University of Grenoble, BP 53, 38041 Grenoble Cedex 9, France, and Bioscience Division, Los Alamos National Laboratory, Los Alamos, New Mexico 87545

Received July 3, 2003; E-mail: langan_paul@lanl.gov

Abstract: The crystal and molecular structure, together with the hydrogen-bonding system in cellulose I_α, has been determined using atomic-resolution synchrotron and neutron diffraction data recorded from oriented fibrous samples prepared by aligning cellulose microcrystals from the cell wall of the freshwater alga *Glaucozystis nostochinearum*. The X-ray data were used to determine the C and O atom positions. The resulting structure is a one-chain triclinic unit cell with all glucosyl linkages and hydroxymethyl groups (*tg*) identical. However, adjacent sugar rings alternate in conformation giving the chain a cellobiosyl repeat. The chains organize in sheets packed in a "parallel-up" fashion. The positions of hydrogen atoms involved in hydrogen-bonding were determined from a Fourier-difference analysis using neutron diffraction data collected from hydrogenated and deuterated samples. The differences between the structure and hydrogen-bonding reported here for cellulose I_α and previously for cellulose I_β provide potential explanations for the solid-state conversion of I_α → I_β and for the occurrence of two crystal phases in naturally occurring cellulose.

Introduction

Although the crystal structure of cellulose has been investigated for almost a century,^{1–5} certain details remain to be deciphered. The molecule in cellulose is a linear polymer of β(1→4) linked D glucosyl residues. In native cellulose (cellulose I), these molecules are synthesized in a continuous fashion by terminal complexes (TC) containing a number of cellulose synthases assembled in biological spinnerets at the cell membrane. Each TC spins a crystalline microfibril consisting of parallel, hydrogen-bonded molecules. In some plants, such as ramie or flax, the microfibrils are generated and assembled in the direction of the plant fiber. Such fibers yield X-ray diffraction patterns with particularly high orientation and resolution. Fiber diffraction studies of these samples have provided crystal structures for cellulose I.^{6,7} However, these structures have been unable to account for all of the diffraction features recorded from samples of oriented cellulose I from algae.⁸

It has subsequently been discovered that the ultrastructure of cellulose possesses unexpected complexity in the form of two crystal phases, namely I_α and I_β.⁹ I_α and I_β can be found not only within the same cellulose sample,¹⁰ but also along a given microfibril.¹¹ The relative amounts of I_α and I_β have been found to vary between samples from different origins. Whereas I_α rich specimens have been found in the cell wall of some algae and in bacterial cellulose, I_β rich specimens have been found in cotton, wood and ramie fibers.^{12,13} The presence of dimorphism, to a large extent, accounts for the initial difficulties in interpreting X-ray fiber and electron diffraction patterns from algal samples. Unraveling the properties of cellulose I therefore requires the determination of not one, but two crystal structures. However, separating the X-ray data collected from mixed-phase samples into I_α and I_β subsets is hazardous. Fiber samples typically correspond to microcrystallites preferentially aligned along the fiber axis, but with random orientation around this axis. One of the consequences of this cylindrical averaging is that reflection spots tend to overlap in fiber diffractograms, making it almost impossible to reliably separate reflections from different phases.

[†] Department of Biomaterial Sciences, Graduate School of Agriculture and Life Science, the University of Tokyo.

[‡] Wood Research Institute, Kyoto University.

[§] Centre de Recherches sur les Macromolécules Végétales, CNRS, affiliated with the Joseph Fourier University of Grenoble.

^{||} Bioscience Division, Los Alamos National Laboratory.

(1) Nishikawa, S.; Ono, S. *Proc. Tokyo Math. Phys. Soc.* **1913**, 7, 131.
(2) Meyer, K. H.; Mark, H. *Ber. Dtsch. Chem. Ges.* **1928**, 61, 593.
(3) Meyer, K. H.; Misch, L. *Helv. Chim. Acta* **1937**, 20, 232.
(4) Gardner, K. H.; Blackwell, J. *Biopolymers* **1974**, 13, 1975.
(5) Sarko, A.; Muggli, R. *Macromolecules* **1974**, 7, 486.
(6) French, A. D. *Carbohydr. Res.* **1978**, 61, 67.
(7) Woodcock, C.; Sarko, A. *Macromolecules* **1980**, 13, 1183.

(8) Honjo, G.; Watanabe, M. *Nature* **1958**, 181, 326.

(9) Atalla, R. H.; VanderHart, D. L. *Science* **1984**, 223, 283.

(10) Sugiyama, J.; Okano, T.; Yamamoto, H.; Horii, F. *Macromolecules* **1990**, 23, 3196.

(11) Sugiyama, J.; Vuong, R.; Chanzy, H. *Macromolecules* **1991**, 24, 4168.

(12) Horii, F.; Hirai, A.; Kitamaru, R. *Macromolecules* **1987**, 20, 2117. (These authors refer to I_α and I_β to distinguish respectively the ramie and cotton family from that of *Valonia* and bacterial cellulose).

(13) Sugiyama, J.; Persson, J.; Chanzy, H. *Macromolecules* **1991**, 24, 2461.

Progress toward resolving this problem has been made in electron diffraction studies of individual cellulose microcrystals extracted from the alga *Microdictyon tenuius*.¹¹ Diffractograms revealed the presence of two distinct crystal phases, a major component with a one-chain triclinic unit cell and a minor component with a monoclinic two-chain unit cell. The major and minor components were shown to correspond to the I_α and I_β phases previously identified in ^{13}C NMR⁹ and FT-IR¹³ studies, respectively. It has also been shown that I_α is metastable and can be converted into I_β by annealing.¹⁴ Additional progress has been made with the discovery that tunicin (cellulose from the small sea animal *Halocynthia roretzi*) consists of nearly pure ($\sim 90\%$) I_β phase,^{15,16} whereas the cellulosic wall of the freshwater alga *Glaucozystis* consists of nearly pure ($\sim 90\%$) I_α phase.¹⁷

Both tunicin and *Glaucozystis* cellulose consist of highly crystalline microfibrils, but these microfibrils are not sufficiently oriented, as in ramie or flax, for fiber diffraction studies: they have an helical organization in tunicin^{18,19} and a curved structure in the cell wall of *Glaucozystis*.²⁰ In view of this difficulty, a method was developed whereby the microfibrils were first hydrolyzed into whiskerlike microcrystals, which were further re-assembled into oriented films amenable to fiber diffraction analyses.²¹ Samples of both I_α and I_β have been prepared in this manner that diffract synchrotron X-rays to atomic resolution,²² allowing the precise location of carbon and oxygen atoms. A method was also devised for replacing all hydrogen atoms involved in hydrogen bonding by deuterium atoms²³ so that their positions could be determined using neutron diffraction.²⁴ The deuterated samples diffract neutrons to resolutions comparable to those obtained with synchrotron X-rays. The determination of the crystal structure and hydrogen-bonding arrangement in cellulose I_β has already been reported.²⁴ In this work, we describe the crystal structure and hydrogen-bonding arrangement in cellulose I_α .

Although we report here the first crystallographic structure for cellulose I_α , there have been several structures predicted from modeling studies.^{25–27} The availability, for the first time, of crystallographic coordinates for both I_α and I_β allows a detailed comparison of the structures and hydrogen-bonding arrangements in these two phases. It allows us to discuss possible routes for the solid-state conversion of I_α to I_β . It also contributes toward a scientific basis for addressing the central issue of why these two phases coexist in nature.

Table 1. Experimental Details

	X-ray	neutron
	crystal data	
chemical formula	$\text{C}_{12}\text{H}_{20}\text{O}_{10}$	$\text{C}_{12}\text{H}_{14}\text{D}_6\text{O}_{10}$
cell setting, space group	triclinic, P1	triclinic, P1
$a(\text{Å})$	6.717(7)	6.717(7)
$b(\text{Å})$	5.962(6)	5.962(6)
$c(\text{Å})$	10.400(6)	10.400(6)
$\alpha(^{\circ})$	118.08(5)	118.08(5)
$\beta(^{\circ})$	114.80(5)	114.80(5)
$\gamma(^{\circ})$	80.37(5)	80.37(5)
$V(\text{Å}^3)$	333.3(6)	333.3(6)
Z	1	
radiation type	synchrotron X-ray	neutron
$\lambda(\text{Å})$	0.72060	1.30580
	data collection	
diffractometer	ID2A	D19
independent reflections	255	158
reflections $> 2\sigma(I)$	236	159
$\theta_{\text{max}}(^{\circ})$	21.10	16.49
range of h	$-6 \rightarrow 5$	$-5 \rightarrow 5$
range of k	$-8 \rightarrow 8$	$-8 \rightarrow 8$
range of l	$-8 \rightarrow 8$	$-8 \rightarrow 8$
refinement		
refinement on	F^2	F^2
$R[F^2 > 2\sigma(F^2)]$	0.1779	0.2049
$\omega R(F^2)$	0.4296	0.4566
$\Delta\rho_{\text{max}}$	0.850	1.552
$\Delta\rho_{\text{min}}$	-0.768	-1.336
ρ_{rms}	0.192	0.414

Experimental Section

Glaucozystis nostochinearum, obtained from the IAM culture collection of the University of Tokyo, was cultivated, and its cellulose extracted, purified, and hydrolyzed using previously described techniques.¹⁷ After conventional washing by centrifugation followed by dispersion in distilled water, the sample consisted of whiskerlike microcrystals having no more than 20 nm in diameter and several micrometers in length (illustrated in Figure 1a). Each of these microcrystals yielded spot electron diffraction diagrams (inserts in Figure 1a) indicating that they corresponded essentially to the triclinic I_α phase. In addition, a rotation about the long axis of a given crystal allowed all sections of the reciprocal lattice to be recorded (exemplified by the two inserts in Figure 1a, which are rotated about the crystal axis by 60° with respect to one another). Following a previously described protocol,^{21,28} the microcrystal suspension was cast as films in which the microcrystals were oriented parallel to one another. These films were used for synchrotron X-ray diffraction experiments, or after deuterium exchange for neutron diffraction experiments.

A typical X-ray diffraction diagram is illustrated in Figure 1b. This diagram, together with a number of others, indicates that the samples are not truly symmetric about the fiber axis, but textured. Special strategies developed for textured cellulose I_β samples were used to collect the X-ray and neutron data from cellulose I_α .²⁴ Neutron data were collected from both hydrogenated and deuterated samples (Figure 1c). Reflection positions and intensities were fitted as described previously,²⁹ with the exception that the orientation of the c^* axis, having refined the positions of the a^* and b^* axes from the equatorial reflection positions, was determined by a grid search using a penalty function $\sum(d^*_o - d^*_c)^2$ where d^*_c is the closest calculated reciprocal reflection spacing from the observed one d^*_o , and the summation is over all reflections. The experimental parameters are summarized in Table 1. It was found that the exact values of the refined unit cell parameters varied as a function of angle around the fiber axis, probably as a result of internal strain within the constituent films and perhaps also due to slightly ex-centric rotation of the sample during data

(14) Horii, F.; Yamamoto, H.; Kitamaru, R.; Tanahashi, M.; Higuchi, T. *Macromolecules* **1987**, *20*, 2946.

(15) Belton, P. S.; Tanner, S. F.; Cartier, N.; Chanzy, H. *Macromolecules* **1989**, *22*, 1615.

(16) Larsson, P. T.; Westermark, U.; Iversen, T. *Carbohydr. Res.* **1995**, *278*, 339.

(17) Imai, T.; Sugiyama, J.; Itoh, T.; Horii, F. *J. Struct. Biol.* **1999**, *127*, 248.

(18) VanDaele, Y.; Revol, J.-F.; Gaill, F.; Goffinet, G. *Biol. Cell* **1992**, *76*, 87.

(19) Gubb, D. *Tissue & Cell* **1975**, *7*, 19.

(20) Willison, J. H. M.; Brown, R. M. *J. Cell. Biol.* **1978**, *77*, 103.

(21) Nishiyama, Y.; Kuga, S.; Wada, M.; Okano, T. *Macromolecules* **1997**, *30*, 6395.

(22) Nishiyama, Y.; Okano, T.; Langan, P.; Chanzy, H. *Int. J. Biol. Macromolecules* **1993**, *26*, 279.

(23) Nishiyama, Y.; Isogai, A.; Okano, T.; Müller, M.; Chanzy, H. *Macromolecules* **1999**, *32*, 2078.

(24) Nishiyama, Y.; Langan, P.; Chanzy, H. *J. Am. Chem. Soc.* **2002**, *124*, 9074.

(25) Aabloo, A.; French, A. D.; Mikelsaar, R. H.; Pertsin, A. J. *Cellulose* **1994**, *1*, 161.

(26) Heiner, A. P.; Sugiyama, J.; Telleman, O. *Carbohydr. Res.* **1995**, *273*, 207.

(27) Vietor, R. J.; Mazeau, K.; Lakin, M.; Perez, S. *Biopolymers* **2000**, *54*, 342.

(28) Nishiyama, Y.; Langan, P.; Chanzy, H. *Fiber Diffraction Rev.* **2003**, *11*, 75.

(29) Nishiyama, Y.; Langan, P. *Fiber Diffraction Rev.* **2000**, *9*, 18.

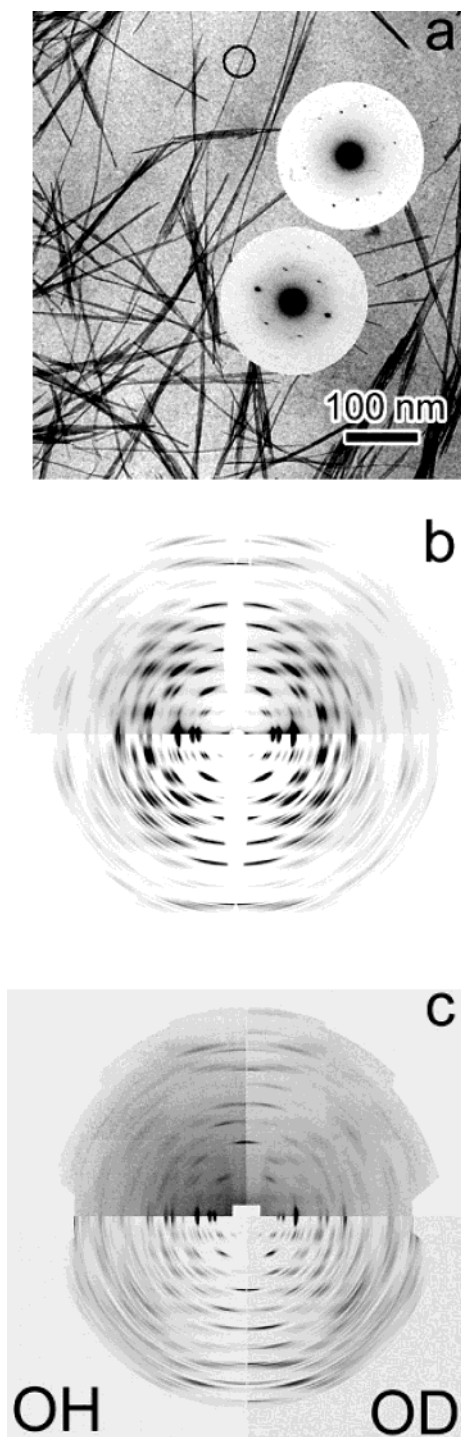


Figure 1. **1a:** Electron micrograph of cellulose microcrystals resulting from the acid hydrolysis of *Glaucozystis* cell wall. When microcrystal areas such as the circled one are probed by electron diffraction, each area yields spot diffraction diagrams (inserts) indicating that the crystals diffract in the I_a triclinic system. The two inserts in (a) were obtained by rotating the crystal by 60° about its long axis. **1b:** (Top) Synchrotron X-ray diffraction data collected on an online MAR image plate from fibers of *Glaucozystis* cellulose I_a on station ID2A at the ESRF, Grenoble, France. (Bottom) A 3D fit of the Bragg intensities, done using custom-written software that takes into account fiber texture. The images have been remapped into cylindrical reciprocal space with the fiber axis vertical. **1c:** (Top) Neutron fiber diffraction patterns collected from two fibers of *Glaucozystis* cellulose I_a , one hydrogenated (left-hand quadrant) and the other deuterated (right-hand quadrant). The bottom quadrants show 3D fits of the Bragg intensities, done using custom-written software that takes into account fiber texture. The images have been remapped into cylindrical reciprocal space with the fiber axis vertical.

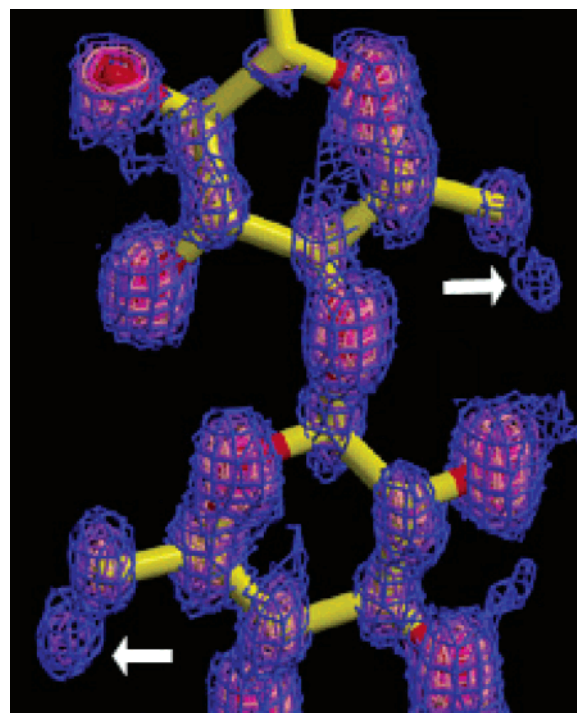


Figure 2. Section through an Omit map calculated using the observed amplitudes and model phases but omitting the hydroxymethyl group oxygen atoms from the phase calculation. The skeletal model represents the cellulose chain. The map is represented at two contour levels in blue and pink. Density (indicated by arrows) can be clearly associated with the hydroxymethyl group in the tg position.

collection. The magnitude of this variation is a fraction of a percent for all unit cell parameters and the unit cell parameters reported in Table 1, are the averages.

Structure Refinement. X-ray structure refinement was carried out using previously described strategies for applying *SHELX-97*³⁰ to high-resolution fiber diffraction data.³¹ Atomic starting positions were taken from the average chain conformation in the crystal structure of cellulose I_β ²⁴, and the chains were arranged in a “parallel-up” fashion.³² An initial refinement was carried out with the hydroxymethyl group atoms removed. The corresponding calculated Omit map showed no sign of hydroxymethyl group disorder and clearly indicated that both groups were in the tg ³³ conformation, Figure 2. The subsequent refinement of all atomic positions, with the exception of hydrogen atoms on hydroxyl groups, with global scaling and thermal parameters, involved a total of 68 parameters, 65 restraints and resulted in values of 17.79% and 42.96% for R and R_w , respectively.³⁴ Allowing individual thermal parameters to refine did not significantly improve the agreement with the data. The coordinates of the final model are given in the crystallographic information file supplied as Supporting Information.

(30) Sheldrick, G. M., *SHELX-97*, a program for the refinement of Single-Crystal Diffraction Data; University of Göttingen: Göttingen, Germany, 1997.

(31) Langan, P.; Nishiyama, Y.; Chanzy, H. *Biomacromolecules* **2001**, *2*, 410.

(32) Koyama, M.; Helbert, W.; Imai, T.; Sugiyama, J.; Henriessat, B. *Proc. Natl. Acad. Sci. U.S.A.* **1997**, *94*, 9091.

(33) The glycosidic torsion angles, Φ and Ψ which describe the relative orientation of adjacent glycosyl residues in the same chain are defined by (O5–C1–O1–C4) and (C1–O1–C4–C5), respectively. The glycosidic bond angle, τ is defined by (C1–O4–C4). The conformation of the hydroxymethyl group is defined by two letters, the first referring to the torsion angle χ (O5–C5–C6–O6) and the second to the torsion angle χ' (C4–C5–C6–O6). An ideal tg conformation would be defined as the set of two angles 180° , -60° .

(34) R is calculated from $\sum(|F_o| - |F_c|)/\sum|F_o|$ with $F_o > 4\sigma$, where F_o and F_c are the observed and calculated amplitudes, respectively. R_w is calculated from $[\sum\omega(F_o^2 - F_c^2)^2/\sum\omega(F_o^2)^2]^{1/2}$, where ω is a weight ($1/\sigma^2$) applied to each F^2 term in the least squares refinement. R_w will be more than twice the size of the R .

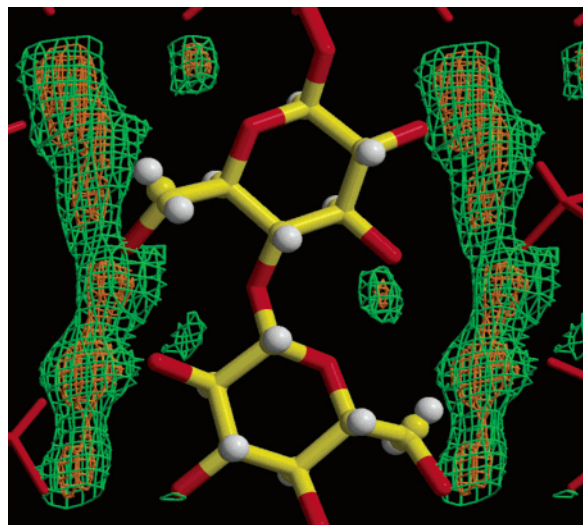


Figure 3. Section through the Fourier difference synthesis calculated with coefficients $(F_d - F_h)\exp i\alpha_c$, where F_d and F_h are the observed structure factor amplitudes from deuterated and hydrogenated cellulose I α , respectively, and α_c are phases calculated from the X-ray structure reported here. The skeletal model represents the cellulose chain. The difference density is represented at two contour levels in green and magenta.

Neutron difference amplitudes, $F_d - F_h$, were combined with phases calculated from the X-ray structure in a Fourier difference synthesis, where F_d and F_h correspond to amplitudes collected from the deuterated and hydrogenated samples, respectively. Labile deuterium atoms on hydroxyl groups were identified with difference density peaks in the synthesis and their positions were subsequently refined using *SHELX-97* and previously described strategies.²⁴ Well-defined difference density peaks, shown in Figure 3, could be clearly identified with one possible deuterium atom position on the secondary alcohol O3 atoms and two possible deuterium atom positions each for the primary alcohol O6 and secondary alcohol O2 atoms. The atom labels are as in Nishiyama et al.,²⁴ with the exception that they are post-fixed with “u” or “d” to associate them with either one of the two independent glucosyl residues. The two partial deuterium atom positions associated with O2u, designated D2uA and D2uB, had their total occupancy constrained to unity and likewise for the partial positions associated with O2d, O6u and O6d, namely, D2dA, D2dB, D6uA, D6uB, D6dA, and D6dB, respectively. However there was no restraint imposed between deuterium atoms associated with different oxygen atoms. The resulting values for R and R_w were 20.41% and 45.33%.

The refined positions of partial deuterium atoms labeled A and B corresponded to those of two intra-sheet hydrogen-bonding networks, also observed in cellulose I β where they were designated I and II.²⁴ When I and II were made mutually exclusive by constraining the deuterium A atoms to have equal occupancy and the occupancy of deuterium A and B atoms to add to unity, the resulting values for R and R_w were 20.49% and 45.66% with a reduction of 3 in the number of parameters. This constrained refinement could not be rejected even at a 50% level of confidence with respect to the previous refinement, and we therefore take it as our best structure. When only A or B atoms were included in the refinement, the resulting values for R and R_w were 21.69% and 49.77%, and 23.65% and 52.53%, respectively. Both these refinements could be rejected with respect to the previous refinement at a confidence level of greater than 97.5%. The refined coordinates and occupancies of the hydrogen atoms are given in the crystallographic information file supplied as Supporting Information. The hydrogen bonding parameters are given in Table 2.

Results and Discussion

The unit cell parameters reported here are slightly smaller and, we believe, more accurate than those deduced from electron

Table 2. Hydrogen Bonds with $H\cdots A < R(A) + 2.800$ Angstroms and $\langle DHA \rangle 110^\circ$

D-H	d(D-H)	d(H \cdots A)	\angle DHA	d(D \cdots A)	A
O3d-D3d	0.989	1.954	163.94	2.918	O5u [x-1, y, z]
O3d-D3d	0.989	2.386	119.05	2.994	O1u [x-1, y, z]
O2d-D2dA	0.974	1.689	133.83	2.465	O6u
O2d-D2dB	0.983	2.283	116.94	2.866	O3d
O2d-D2dB	0.983	2.679	157.47	3.606	O6d [x, y-1, z+1]
O2u-D2uA	0.980	1.763	127.07	2.480	O6d [x+1, y, z]
O2u-D2uA	0.980	2.181	118.44	2.784	O1u
O2u-D2uB	0.985	2.357	110.37	2.853	O3u
O2u-D2uB	0.985	3.019	122.21	3.641	O6u [x, y+1, z-1]
O6d-D6dA	0.977	2.176	122.20	2.821	O3d [x, y+1, z-1]
O6d-D6dA	0.977	2.791	141.32	3.606	O2d [x, y+1, z-1]
O6d-D6dB	0.976	1.894	150.36	2.785	O1u [x-1, y, z]
O6d-D6dB	0.976	1.967	110.23	2.480	O2u [x-1, y, z]
O6u-D6uA	0.983	1.853	153.99	2.770	O3u [x, y-1, z+1]
O6u-D6uA	0.983	2.881	134.82	3.641	O2u [x, y-1, z+1]
O6u-D6uB	0.976	1.956	145.03	2.812	O1d
O3u-D3u	0.976	2.072	137.59	2.868	O5d

diffraction experiments.¹¹ The mass densities calculated from the parameters reported in this study and the electron diffraction study are 1.61 and 1.58, respectively. Electron beams are known to damage polymer crystals by inducing cross-links and chemical modifications. In the case of cellulose, it has been reported that this damage results in a swelling of the crystal cell and therefore a reduction in crystal density.^{35,36}

Selected model parameters for I α and I β are given in Table 3. In I β , there are two conformationally distinct chains in a monoclinic $P2_1$ unit cell, referred to as the corner and center chains. Each chain lies on $P2_1$ symmetry axis that requires adjacent glucosyl residues in the same chain to be identical. In I α , there is one chain in a triclinic unit cell, and no requirement for adjacent glucosyl residues in that chain to be identical. The relative orientation of adjacent glucosyl residues can be described by the glucosidic torsion angles Φ and Ψ , the bond angle τ , and the conformation of hydroxymethyl groups can be described by torsion angles χ and χ' .³³ The values of the parameters in Table 3 are all well within the ranges observed in crystals of small analogues of cellulose.³⁷

Whereas the conformations of the symmetry independent glucosidic linkages and hydroxymethyl groups are different in I β , they are identical to within experiment error in I α . However, the conformations of the symmetry independent sugar rings, represented by the calculated Cremer and Pople puckering parameter θ , are different in both I α and I β .³⁸ These results are in agreement with recent CP/MAS ¹³C NMR studies of cellulose and cellulose derivatives. Horii et al.^{39,40} have shown that there is a correlation between the chemical shifts in CP-MAS spectra and the dihedral angles defined by the bonds associated with that particular carbon atom. In precisely assigning the chemical shifts of the sugar carbon atoms in I α and I β , it has been shown by Kono et al.^{41,42} that there are two nonequivalent gluco-

(35) Revol, J. F. *J. Mater. Sci.* **1985**, *4*, 1347.

(36) Sugiyama, J.; Okano, T. In *Cellulose Structure and Functional Aspects*; Kennedy, J. F.; Phillips, G. O.; William P. A. Eds.; Ellis Horwood Publishers: Manchester 1989; p. 75.

(37) French, A. D.; Johnson, G. P. *Cellulose*, in press.

(38) Cremer, D.; Pople, J. A. *J. Am. Chem. Soc.* **1975**, *97*, 1354.

(39) Horii, F.; Hirai, A.; Kitamaru, R. *Polym. Bull.* **1983**, *10*, 357.

(40) Horii, F.; Hirai, A.; Kitamaru, R. In *Polymers for Fibers and Elastomers*; Arthur Jr, J. C., Ed.; ACS Symposium Series 260, *J. Am. Chem. Soc.*, Washington, D. C. 1984; p.27.

(41) Kono, H.; Erata, T.; Takai, M. *Macromolecules* **2003**, *36*, 3589.

(42) Kono, H.; Yunoki, S.; Shikano, T.; Fujiwara, M.; Erata, T.; Kawai, M. *J. Am. Chem. Soc.* **2002**, *124*, 7506.

Table 3. Selected Model Parameters^a

	residue 1						residue 2					
	Φ	Ψ	τ	χ	χ'	θ	Φ	Ψ	τ	χ	χ'	θ
I_α	-98 (3)	-138 (2)	116	167 (3)	-75 (4)	9.4	-99 (3)	-140 (3)	116	166 (3)	-74 (4)	6.9
I_β	-98.5 (20)	-142.3 (19)	115	170 (3)	-70 (3)	10.2	-88.7 (20)	-147.1 (16)	116	158 (3)	-83 (3)	6.7

^a Residue 1 corresponds to the origin chain in cellulose I_β and the “d” residue in cellulose I_α . Residue 2 corresponds to the center chain in cellulose I_β and the “u” residue in cellulose I_α . The values in parentheses are experimental standard deviations on the corresponding last digit places.

pyranosyl residues in the unit cells of both allomorphs, in agreement with the results presented here. Furthermore, Kono et al. have shown that the main differences between the I_α and I_β structures are in the conformations of the anhydroglucose residues and the β -1,4 linkages.⁴² The list of conformational parameters presented in Table 3 is in full agreement with the NMR results of Kono et al.⁴²

The chemical shifts of the C6 resonance can be correlated with χ and χ' ,³⁹ and the chemical shifts associated with C1 and C4 can be correlated with Φ and Ψ , respectively.⁴⁰ The fact that the C6 and C1 resonances are observed as single peaks in I_α spectra but are distinctly split in I_β spectra is in agreement with the results presented here. Because the C4 resonance is split in both I_α and I_β spectra one would expect there to be two distinct values of Ψ in I_α and I_β . Although this is the case in I_β , in I_α the values of this torsion angle are equal to within experimental error. One explanation for this is that the C4 chemical shift is extremely sensitive to changes in local conformation to a degree beyond the accuracy of this study. In particular, the two symmetry independent (C1–O1–C4–C5) torsion angles -138 (3)° and -140 (3)° could possibly differ by more than 8°.

As with cellulose I_β , there is no hint of inter-sheet O–H...O hydrogen bonds in cellulose I_α . Within each sheet the neutron Fourier difference maps indicate that although the hydrogen atoms associated with O3 occupy single well-defined positions the hydrogen atoms associated with O2 and O6 are distributed between a number of partially occupied, but still well-defined, positions. As with cellulose I_β , these partially occupied positions can be described by two mutually exclusive hydrogen-bonding networks, designated I and II.²⁴ It was previously noted that the situation in reality may correspond to a dynamic balance between I and II, I and II may coexist in different parts of the sample, or the situation may be more complicated with local hydrogen bonding geometries changing in both position and time. However, it is convenient to use the concept of two exclusive networks here for the purpose of comparing hydrogen bond geometries in cellulose I_α and I_β .

In both cellulose I_α and I_β , there are relatively strong O3–H...O5 intrachain hydrogen bonds. In cellulose I_β there is an alternation in these bonds between the origin and center chains (H...A are 1.966 Å, 1.752 Å, \angle DHA are 137.08°, 162.23° for origin and center chain respectively). In cellulose I_α there is a similar alternation but this time down the same chain (H...A are 2.072 Å, 1.954 Å and \angle DHA 137.59°, 163.94°). In network I, the intrachain O2–H...O6 bond distances are shorter in I_α compared to I_β (H...A are 1.689 Å, 1.763 Å for I_α and 1.832, 1.904 in I_β) and the interchain O6–H...O3 bond distances are shorter in I_β compared to I_α (H...A are 1.853 Å, 2.176 Å for I_α and 1.779 Å, 2.040 Å in I_β). However, for both of these types of bonds the angles are much closer to 180° in I_β compared to

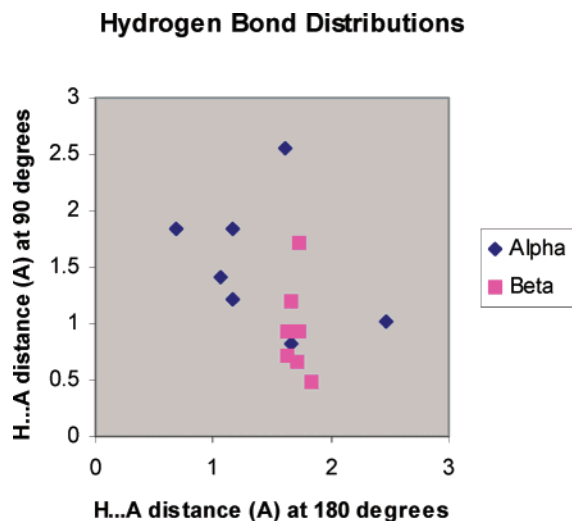


Figure 4. Distribution of H...A bond distances and \angle DHA bond angles for O2 and O6 donors in cellulose I_α (blue) and I_β (pink). Each point represents a hydrogen bond. The distance of the point from the origin represents the H...A distance and the anticlockwise rotation of point away from the x-axis about the origin represents $180^\circ - \angle$ DHA

I_α (\angle DHA are 133.83°, 127.07°, 122.20°, and 153.99° in I_α and 158.72°, 144.26°, 165.12° and 156.61° in I_β). Many of these bonds are bifurcated in I_α and I_β with similar types of minor components.

In network II, there is only one instance of the intrachain O6–H...O2 bond in I_α and two in I_β . However there are two instances of the interchain O2–H...O6 bond in I_α and only one in I_β . The network II bond distances are shorter (H...A are 2.679 Å, 3.019 Å and 1.967 Å in I_α and 1.876 Å, 2.440 Å, and 1.967 in I_β) and the bond angles larger (\angle DHA are 157.47°, 122.21°, and 110.23° in I_α and 150°, 152.06° and 135.44° in I_β) in I_β compared to I_α .

Jeffrey has used the concept of strong, moderate and weak hydrogen bonds in order to explain observed hydrogen bonding geometries.⁴³ The H...A distances are 1.2–1.5 Å, 1.5–2.2 Å, and 2.2–3.2 Å for strong, medium and weak bonds and the bond angles are 175°–180°, 130°–180° and 90°–150°, respectively. Desiraju and Steiner have used two categories to describe hydrogen bonds, strong and weak, where H...A is 1.5–2.2 Å and 2.2–3 Å for strong and weak bonds and the bond angles are 130°–180° and 90°–180°, respectively.⁴⁴ The geometries of the major hydrogen bond components involving O2 and O6 donors in I_α and I_β are represented visually in Figure 4. Most of the hydrogen bonds are of the moderate type according to Jeffrey and the strong type according to Desiraju

(43) Jeffrey, G. A. *An Introduction to Hydrogen Bonding*; Oxford University Press: Oxford, U.K., 1997.

(44) Desiraju, G. R.; Steiner, T. *The Weak Hydrogen Bond*; Oxford University Press: New York, 1999.

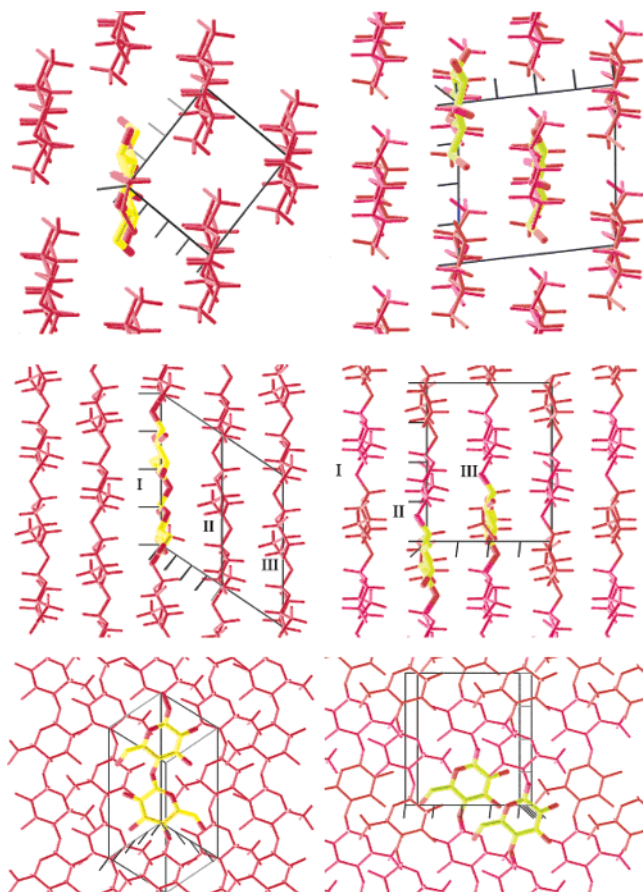


Figure 5. Projections of the crystal structures of cellulose I α (left) and I β (right) down the chain axes (top), perpendicular to the chain axis and in the plane of the hydrogen bonded sheets (middle), and perpendicular to the hydrogen bonded sheets (bottom). The cellulose chains are represented by red skeletal models. The asymmetric unit of each structure is also represented in thicker lines with carbons in yellow. The unit cell of each structure is shown in white.

and Steiner. However, two hydrogen bonds in I α and one hydrogen bond in I β are weak according to both Jeffrey and Desiraju and Steiner. It is clear from Figure 4 that the hydrogen bonds in I β are distributed over a region of better geometry than those in I α . The more favorable intra-sheet hydrogen bonding in I β must be due to the difference in cellulose chain conformation between I α and I β .

Another difference between the hydrogen bonding in I α and I β is that the relative occupancies of the two networks are different (network I is ~ 70 – 80% occupied in I β and $\sim 55\%$ in I α). The significance of this was tested by repeating the cellulose I α deuterium atom refinement, this time constraining the deuterium A atoms to have an occupancy of 75% as in cellulose I β . The resulting values for R and R ω were 20.79% and 46.63% , respectively. This refinement could be rejected with respect to the previous refinements at a confidence level of greater than 97.5% .

In summary, the intra-sheet hydrogen bonding involving O2 and O6 donors is disordered over two possible networks in both cellulose I α and I β . The geometry of these networks is better in I β than in I α . The occupancy of these networks is different in I α and I β . The strong intrachain O3–H \cdots O5 hydrogen bonds that give the cellulose chains their ribbon shape alternate between two slightly different geometries in both cellulose I α and I β . In

cellulose I α the alternation is down the same chain. In cellulose I β the alternation is between conformationally distinct chains.

The projections of the crystal structures of cellulose I α and I β down the chain axes are remarkably similar, Figure 5. As the projection perpendicular to the chain axis and in the plane of the hydrogen bonded sheets shows, the main difference between I α and I β is the relative displacement of the sheets in the chain direction. In both I α and I β , the second sheet, designated II, is shifted in the “up” direction by $\sim c/4$ relative to the first sheet, designated I. The third sheet, designated III, is similarly shifted with respect to II by $\sim c/4$ in I α but in I β it is shifted by a $\sim c/4$ in the “down” direction. There is a relative difference of $\sim c/2$ in the position of III with respect to II in I α and I β . Because there exists an approximate molecular 2_1 screw axis, this difference is equivalent to stacking opposite faces of III on II.

The most likely route for solid-state conversion of cellulose I α \rightarrow I β is the relative slippage of the cellulose chains past one another.⁴⁵ This movement does not require the disruption of the hydrogen-bonded sheets (along the 100 planes for cellulose I β and 110 planes for cellulose I α) but slippage by $\sim c/2$ at the interface of sheets of type II and III in Figure 5. We note that there is also the possibility that the chains in III could rotate around their axes, because a slippage of $\sim c/2$ is equivalent to a rotation of 180° around a 2_1 molecular axis. However this seems unlikely.

It has been hypothesized that the inner cohesion of ambient cellulose crystals is largely due to the van der Waals attraction between hydrogen-bonded sheets.^{46,47} Despite the apparent strength of these interactions at room temperature, they are clearly effected by heating the crystals; the lattice is remarkably constant in directions within the hydrogen-bonded sheets, but expands in the stacking direction.⁴⁸ Wada has recently observed a new phase in cellulose at temperatures higher than $220/230^\circ\text{C}$, where the conversion I α \rightarrow I β takes place.⁴⁹ Little is known about this phase except that it corresponds to a crystalline structure where the inter-sheet distance has expanded by about 6% , whereas distances within the sheets are essentially constant.

A recent study of α -glycine suggests a possible mechanism for this anisotropic thermal expansion. In crystals of α -glycine, molecules are arranged in hydrogen-bonded sheets with the molecular axes lying within the sheets.⁵⁰ On heating, the unit cell expands anisotropically with the stacking direction increasing the most. The increasing separation of the sheets is driven by an increase in molecular libration about an axis that lies in the plane of the sheets and which causes the movement of atoms out of this plane. There is a corresponding weakening of the inter-sheet bonding interactions. It is possible that librations of the cellulose chains about axes that lie in the plane of the hydrogen-bonded sheets is the driving mechanism for sheet separation, and lubrication, during conversion of I α \rightarrow I β .

Although van der Waals attraction between hydrogen-bonded sheets may well contribute to cellulose crystal cohesion our results indicate that weak C–H \cdots O hydrogen bonding also plays

(45) Hardy, B. J.; Sarko, A. *Polymer* **1996**, *37*, 1833.

(46) French, A. D.; Miller D. P.; Aabloo, A. *Int. J. Biol. Macromol.* **1993**, *15*, 30.

(47) Cousins, S. K.; Brown, R. M. Jr. *Polymer* **1995**, *36*, 3885.

(48) Wada, M.; Kondo, T.; Itoh, T. *Polym. J.* **2003**, *35*, 155.

(49) Wada, M. *J. Polym. Sci., Part B: Polym. Phys.* **2002**, *40*, 1095.

(50) Langan, P.; Mason, S. A.; Myles, D.; Schoenborn, B. P. *Acta Crystallogr.* **2002**, *B58*, 728.

Table 4. Potential Inter-Sheet Weak Hydrogen Bonds with $D\cdots A < r(D) + r(A) + 0.50 \text{ \AA}$ $D(H\cdots A) < r(H) + r(A) - 0.12 \text{ \AA}$ and $D-H\cdots A > 100.0^\circ$ ^a

	D	H	A	H \cdots A	D \cdots A	D-H \cdots A (deg)
I $_{\alpha}$	C2u	H2u	O1d	2.5136	3.40(4)	149.86
I $_{\alpha}$	C6d	H6Au	O2d	2.5078	3.48(5)	176.31
I $_{\alpha}$	C6d	H6Bu	O2d	2.5842	3.43(5)	146.36
I $_{\alpha}$	C6u	H6Au	O5d	2.4738	3.23(4)	134.63
I $_{\beta}$	C1c	H1c	O6o	2.5476	3.3908	144.15
I $_{\beta}$	C2c	H2c	O3o	2.4930	3.4668	172.39
I $_{\beta}$	C3o	H3o	O2c	2.5158	3.4612	162.01
I $_{\beta}$	C5c	H5c	O1o	2.5862	3.4353	145.01
I $_{\beta}$	C6c	H6Ac	O2o	2.3585	3.3232	172.84

^a The values in parentheses are experimental standard deviations on the corresponding last digit places.

a role. Table 4 shows that there are potential weak hydrogen bonds of this type in both I $_{\alpha}$ and I $_{\beta}$. There are more C-H \cdots O inter-sheet bonds in I $_{\beta}$ than in I $_{\alpha}$. The average H \cdots A distances are about the same in I $_{\alpha}$ (2.52 Å) and I $_{\beta}$ (2.50 Å). The bond angles for such weak interactions are probably not so important but they are larger in I $_{\beta}$ (159.28°) than in I $_{\alpha}$ (151.79°). It is likely that enhanced C-H \cdots O interactions contribute to the stability of I $_{\beta}$ over I $_{\alpha}$. Both I $_{\beta}$ and I $_{\alpha}$ also contained short H \cdots H interactions (2.52 Å in I $_{\beta}$ and 2.4 Å and 2.46 Å in I $_{\alpha}$). No attempt was made to relieve these contacts because they are typical for short H \cdots H distances involved in single-crystal studies of cellulose fragments.

As discussed above, the crystallographic structures and hydrogen bonding arrangements for cellulose I $_{\alpha}$ and cellulose I $_{\beta}$ provide important insights into cellulose stability and transformation and contribute toward a scientific basis for understanding cellulose biogenesis and reactivity. However, they also provide the basic parameters required for the application of a number of other techniques to understanding the properties of cellulose. In particular, these results will enable modeling studies of the properties of whole fibers of cellulose, I $_{\alpha}$ /I $_{\beta}$ interfaces within those fibers and the surface properties of

those fibers. These results also provide an important key for interpreting spectroscopic data.

In addition to their practical impact, these results have brought some surprises. In the I $_{\alpha}$ phase, the cellulose molecules adopt a conformation remarkably close to a 2-fold screw, which is not required by the triclinic space group. On the other hand, in the I $_{\beta}$ allomorph, where the 2-fold screw is required by the symmetry, surprising conformational differences exist between the center and the corner chains. The presence of two similar hydrogen bonding networks with different occupancies in cellulose I $_{\alpha}$ and I $_{\beta}$ was not expected. Neither was it expected that there would be an alternation of intrachain O3-H \cdots O5 hydrogen bonds in both phases. At the same time these crystallographic studies were underway, 2D solid-state NMR studies were being carried out by Kono et al on cellulose I $_{\alpha}$ and I $_{\beta}$.⁴² Although these studies were done independently and simultaneously, they have provided remarkably consistent information about cellulose conformation at an unprecedented level of detail. At the start of these studies, not many would have projected that cellulose I $_{\alpha}$ and cellulose I $_{\beta}$ differ to such an extent in crystal packing, molecular conformation and hydrogen bonding.

Acknowledgment. The authors thank the Institut Laue Langevin and the European Synchrotron Radiation Facilities for the provision of beamtime. Y.N. thanks the French Government and the Japanese Society for the Promotion of Science for financial support. P.L. thanks the Office of Science and the Office of Biological and Environmental Research of the US Department of Energy for financial support.

Supporting Information Available: Coordinates of the final model and the refined coordinates and occupancies of the hydrogen atoms are given in a crystallographic information file. This material is available free of charge via the Internet at <http://pubs.acs.org>.

JA037055W